

Green Chemistry

Accepted Manuscript



This article can be cited before page numbers have been issued, to do this please use: Z. Ke, Y. Zhang, X. Cui and F. Shi, *Green Chem.*, 2015, DOI: 10.1039/C5GC01992C.



This is an *Accepted Manuscript*, which has been through the Royal Society of Chemistry peer review process and has been accepted for publication.

Accepted Manuscripts are published online shortly after acceptance, before technical editing, formatting and proof reading. Using this free service, authors can make their results available to the community, in citable form, before we publish the edited article. We will replace this *Accepted Manuscript* with the edited and formatted *Advance Article* as soon as it is available.

You can find more information about *Accepted Manuscripts* in the [Information for Authors](#).

Please note that technical editing may introduce minor changes to the text and/or graphics, which may alter content. The journal's standard [Terms & Conditions](#) and the [Ethical guidelines](#) still apply. In no event shall the Royal Society of Chemistry be held responsible for any errors or omissions in this *Accepted Manuscript* or any consequences arising from the use of any information it contains.



Green Chemistry

ARTICLE

Supported Nano-Gold-Catalyzed N-Formylation of Amines with Paraformaldehyde in Water under Ambient Conditions

Zhengang Ke,^{a,b} Yan Zhang,^a Xinjiang Cui,^a and Feng Shi^{*a}Received 00th January 20xx,
Accepted 00th January 20xx

DOI: 10.1039/x0xx00000x

www.rsc.org/

A simple and efficient Au/Al₂O₃ catalyst was prepared by co-precipitation method for the oxidative N-formylation of amines with paraformaldehyde. Under the optimized reaction conditions, excellent amine conversion and N-formamide selectivity can be obtained with up to 97% yield with water as the solvent under ambient conditions. This catalyst was tolerated a wide scope of primary amines and second amines, and it can be reused for at least five runs without obvious deactivation.

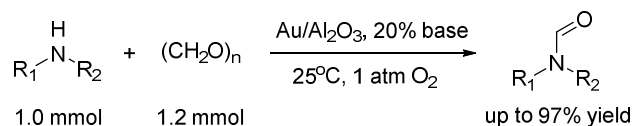
Introduction

Supported nano-gold catalysts have been widely used in various catalytic reactions, e.g. selective hydrogenation, selective oxidation, hydrochlorination of alkynes, carbon monoxide elimination and many others¹⁻³. Gold nano particles can dissociate molecular oxygen to atomic oxygen at low temperature due to its unique surface structure and physicochemical properties⁴. So, supported nano-gold catalyst exhibits excellent catalytic performance in the selective oxidation reactions. Therefore, the applying of supported nano-gold catalyst allows the progress of oxidation reaction at low reaction temperature thus the side reactions can be inhibited. As we all know, selective oxidation reaction constitutes one of the industrial core technologies for converting bulk chemistry to useful products of a higher oxidation state⁵, so nano-gold catalysis presents a good choice in the development of selective oxidation reactions.

N-Formamide is an important class of compounds⁶ which are widely used in organic synthesis and biological intermediates in fungicide⁷, isocyanate⁸, nitrile, and pharmaceuticals synthesis^{9,10}. Traditionally, the N-formamide synthesis involves the use of stoichiometric amounts of coupling reagents, such as a carbodiimide, it makes the reaction operations complicated, and causes equipment corrosion and poor atom-economy¹¹⁻¹³. The direct catalytic synthesis of N-formamide from amines and carbonyl compounds has become a field of emerging importance due to its high atom efficiency. The catalytic N-formylation of amines

has been reported with various carbonyl source reagents such as formic acid or formate¹⁴⁻¹⁸, esters^{19,20}, cyanide²¹⁻²⁹, and oxime³⁰⁻³⁶, CO₂/H₂^{37,38} and methanol³⁹⁻⁴². Notably, formaldehyde as the carbonyl source for N-formamide synthesis has been less studied.

Recently, the direct N-formylation of amines with formaldehyde as the carbonyl source was reported. Originally, the N-formylation of aliphatic amines can be realized with 3.0 equivalent of aqueous formaldehyde or paraformaldehyde at 115 °C in the presence of homogeneous iridium catalyst⁴³. Following several nano-gold catalyst systems were applied in this transformation. For example, N-formylation of amine with 1.5 equiv., formalin in the presence of 1.0 equiv., NaOH can be realized using ethanol/water (1:2) as solvent under aerobic oxidation conditions catalyzed by PVP stabilized gold nano particles⁴⁴. The N-formylation reaction of aromatic amines can also be performed with 2.0 equiv., aqueous formaldehyde solution and 3.0 equiv., NaOH catalyzed by carbon nanotube supported nano-gold catalyst⁴⁵. However, the above reaction systems have one or more shortcomings such as difficulty in separation of catalysts with product, the applying of a great deal of base, excessive amount of formaldehyde, and organic solvent.



Scheme 1. Oxidative N-formylation of amine with paraformaldehyde catalyzed by supported nano-gold catalyst under ambient conditions

In this work, a simple and efficient Au/Al₂O₃ catalyst was developed for the N-formylation reaction of amines with stoichiometric amount of paraformaldehyde applying water as the sole solvent. The N-formylation of aliphatic and aromatic amines with different structures can be realized with excellent

^a State Key Laboratory for Oxo Synthesis and Selective Oxidation, Centre for Green Chemistry and Catalysis, Lanzhou Institute of Chemical Physics, Chinese Academy of Sciences, No. 18, Tianshui Middle Road, Lanzhou, P. R. China. E-mail: fshi@licp.cas.cn.

^b University of Chinese Academy of Sciences, Beijing, 100049.

† Footnotes relating to the title and/or authors should appear here.

Electronic Supplementary Information (ESI) available: [details of any supplementary information available should be included here]. See DOI: 10.1039/x0xx00000x

yields (Scheme 1), and the catalyst can be reused for five runs without obvious deactivation.

Experimental section

All solvents and chemicals were obtained commercially and were used as received.

Catalyst preparation and characterization

The Au/Al₂O₃ was prepared by co-precipitation method. 18 mmol Al(NO₃)₃•9H₂O and 6.9 mL HAuCl₄•4H₂O (10 mg/mL) were added into 120 mL deionized water at rt., under vigorous stirring. Then, 20 mL Na₂CO₃ aqueous solution (1.35 M) was added dropwise to the solution, and the pH value of the final solution was ~7.0. After further stirring for 4 h, the resulting precipitate was separated and washed by deionized water, dried at 100 °C in air for 6 h, calcined at 400 °C for 4 h, and then reduced under hydrogen flow at 350 °C for 3 h. The resulting catalyst samples were denoted as Au/Al₂O₃, Pd/Al₂O₃, Pt/Al₂O₃, Ru/Al₂O₃, Au/FeO_x, Au/NiO_x and Au/CuO_x were prepared with the same procedures.

Following, the catalysts were characterized by inductively coupled plasma-atomic emission spectroscopy (ICP-AES), BET surface-area analysis (BET), transmission electron microscopy (TEM), X-ray powder diffraction (XRD), X-ray photoelectron spectroscopy (XPS), and the reaction products were characterized by nuclear magnetic resonance spectrum (NMR). XRD measurements were conducted by using a STADIP automated transmission diffractometer (STOE) equipped with an incident beam curved germanium monochromator with CuKα1 radiation and current of 40 kV and 150 mA, respectively. The XRD patterns were scanned in the 2 Theta range of 5-100°. XPS were obtained using a VG ES-CALAB 210 instrument equipped with a dual Mg/Al anode X-ray source, a hemispherical capacitor analyzer, and a 5 keV Ar⁺ iron gun. The electron binding energy was referenced to the C1s peak at 284.8 eV. The background pressure in the chamber was less than 10⁻⁷ Pa. The peaks were fitted by Gaussian-Lorentzian curves after a Shirley background subtraction. For quantitative analysis, the peak area was divided by the element-specific Scofield factor and the transmission function of the analyzer. The BET surface area measurements were performed on a Micromeritics 2010 instrument at the temperature of 77 K. The pore size distribution was calculated from the desorption isotherm by using the Barrett, Joyner, and Halenda (BJH) method. Prior to measurements, the samples were degassed at 200 °C for 10 h, at a rate of 10 °C/min. TEM was carried out by using a Tecnai G2 F30 S-Twin transmission electron microscope operating at 300 kV. Single-particle EDX analysis was performed by using a Tecnai G2 F30 S-Twin Field Emission TEM in STEM mode. For TEM investigations, the catalysts were dispersed in ethanol by ultrasonication and deposited on carbon-coated copper grids. NMR spectra were measured by using a Bruker ARX 400 or ARX 100 spectrometer at 400 MHz (¹H) and 100 MHz (¹³C). All spectra were recorded in CDCl₃ and chemical shifts (δ) are reported in ppm relative to tetramethylsilane referenced to the residual solvent peaks.

Catalytic performance test

The catalytic activity was tested by N-formylation of morpholine as the model reaction. 1.0 mmol morpholine, 1.2 mmol paraformaldehyde, 0.2 mmol NaOH and 2 mL deionized water were added to a 38 mL press tube and exchanged with O₂. The reaction was carried out at 25 °C for 6 h with the magnetic stirring speed of 900 rpm. Subsequently, the reaction mixture was diluted with 5 mL methanol for quantitative analysis by GC-MS (Agilent 7890B-5977A). And then, the crude reaction mixture was concentrated by rotary evaporator and purified by column chromatography to give the isolated compound. N-formyl morpholine was obtained and purified by column chromatography, with 97% isolated yields, using dichloromethane/methanol (10 : 1, R_f = 0.77) to give a colorless oil. ¹H NMR (400 MHz, CDCl₃) δ 8.06 (s, 1H), 3.74 – 3.63 (m, 4H), 3.59 (q, J = 4.8 Hz, 2H), 3.45 – 3.35 (m, 2H). ¹³C NMR (100 MHz, CDCl₃) δ 160.82, 67.24, 66.45, 45.80, 40.63.

Results and discussion

Catalyst characterization studies

BET characterization

Table 1. The physical properties of catalysts

Sample	Noble metal Loading/wt% ^[a]	BET surface area/m ² /g ^[b]	Pore volume/cm ³ /g ^[b]
Au/Al ₂ O ₃	2.62	152.8	0.57
Pd/Al ₂ O ₃	3.56	166.0	0.36
Pt/Al ₂ O ₃	1.53	147.7	0.73
Ru/Al ₂ O ₃	1.19	150.4	0.91
Au/FeO _x	3.34	5.8	0.11
Au/NiO _x	3.42	6.4	0.07
Au/CuO _x	3.21	5.0	0.03

[a] Determined by ICP-AES, [b] Determined by IQ2 automated gas sorption analyser.

N₂ adsorption-desorption analysis was used to determine the surface area and structure of the prepared supported catalysts (Table 1, Fig. S1). The catalysts with Al₂O₃ as support provide larger surface areas comparing those with FeO_x, NiO_x and CuO_x as supports. For example, the BET surface areas of Au/Al₂O₃, Pd/Al₂O₃, Pt/Al₂O₃ and Ru/Al₂O₃ are in the range of 147.7-166.0 m²/g, while less than 10 m²/g BET surface areas are observed in catalysts Au/FeO_x, Au/NiO_x and Au/CuO_x. In the meanwhile, the pore volumes were significantly decreased, too. It might be due to the reducibility of FeO_x, CuO_x and NiO_x. Partial reduction of these metal oxides occurred when the catalysts were treated under hydrogen flow at 350 °C. The XRD characterization also reveals the existence of metallic Cu and Ni in the final catalyst samples.

TEM characterization

TEM images of the as-synthesized catalysts samples Au/Al₂O₃, Pd/Al₂O₃, Pt/Al₂O₃, Ru/Al₂O₃, Au/FeO_x, Au/NiO_x and Au/CuO_x are shown in Fig. 1 and Fig. S2. Based on the TEM images of catalyst Au/Al₂O₃, it can be seen that the Au nano-particles were well dispersed on the support (Fig. 1A and H). According to the statistic results of TEM image, the average diameter of gold particles is ~2.5

nm, and 73% of nano-gold particles dropped in the range of 2-3 nm. In catalysts Pd/Al₂O₃ and Pt/Al₂O₃, the nano-Pd and nano-Pt particles were also well dispersed on the surface of Al₂O₃ (Fig. 1B and C), and the mean diameters are ~2.7 nm and ~2.8 nm (Fig. S2A and B). Interestingly, no obvious Ru and Au nanoparticles were observed from the TEM images of Ru/Al₂O₃ and Au/CuO_x.

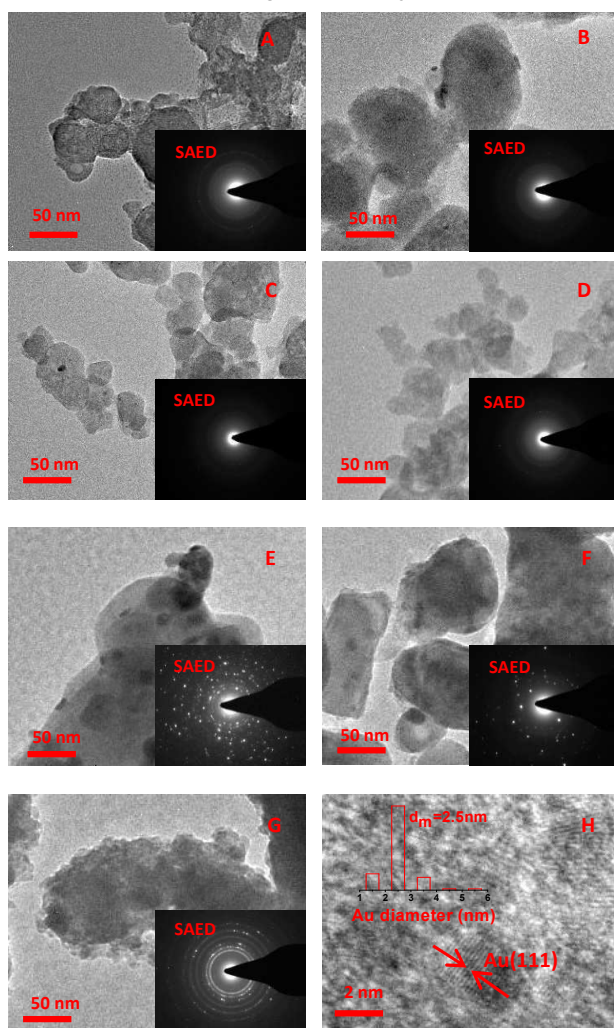


Figure 1. TEM images of supported catalysts samples synthesized with co-precipitation method. (A) Au/Al₂O₃, (B) Pd/Al₂O₃, (C) Pt/Al₂O₃, (D) Ru/Al₂O₃, (E) Au/FeO_x, (F) Au/NiO_x, and (G) Au/CuO_x. Insets: SAED patterns of the corresponding samples.

It suggests that the Ru and Au species might be encapsulated inside the supports or highly dispersed on the supports. Bigger nano-gold particles, with mean diameter of ~8.3 nm and ~9.4 nm were formed if the catalyst supports were FeO_x and NiO_x (Fig. 1E and F and Fig. S2D and E). If taking the results of catalytic performance exploration into consideration together, we can imagine that the coagulation of nano-gold particles in catalysts Au/FeO_x and Au/NiO_x might be one of the reasons for their low activities.

XRD characterization

Fig. 2 shows the XRD diffraction patterns of the as-prepared supported catalysts. Based on the XRD diffraction patterns, the Au/Al₂O₃ sample shows diffraction peaks at 38.3°, 44.3°, 64.7° and 77.5°, which can be ascribed to the diffraction peaks of Au

(111), (200), (220) and (311). However, there are no Pt, Pd and Ru diffraction peak can be observed when Pd/Al₂O₃, Pt/Al₂O₃ and Ru/Al₂O₃ were characterized by XRD. It suggests that Pd, Pt and Ru were well dispersed on the supports and amorphous Pd, Pt and Ru species were formed in the samples. About the diffraction patterns of Au/FeO_x, Au/NiO_x and Au/CuO_x, it can be seen clearly that the diffraction peaks can be attributed to Fe₃O₄, metallic nickel and copper, i.e. 35.5° Fe₃O₄ (311), 62.5° Fe₃O₄ (440), 30.1° Fe₃O₄ (220), 57.0° Fe₃O₄ (511), 42.9° Fe₃O₄ (400); 44.4° Ni (111), 98.4° Ni (222), 76.4° Ni (220), 51.87° Ni (200), 92.9° Ni (311); 50.5° Cu (200), 43.4° Cu (111), 74.0° Cu (220) and 89.9° Cu (311). No characteristic diffraction peak ascribed to noble metal species was observable, indicating that these gold particles were well dispersed and no crystallized gold formed. The metallic copper and nickel species should be formed during the reduction of the catalysts samples.

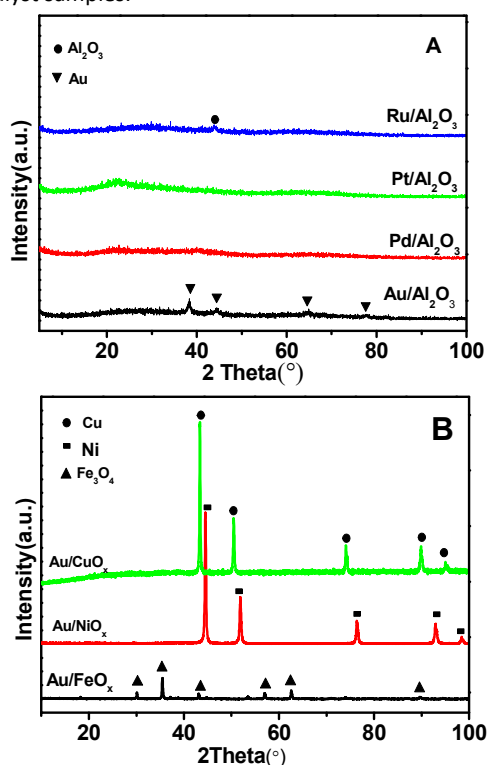


Figure 2. XRD diffraction patterns of catalysts Au/Al₂O₃, Pd/Al₂O₃, Pt/Al₂O₃ (A) and Ru/Al₂O₃, Au/FeO_x, Au/NiO_x and Au/CuO_x (B).

XPS characterization

The catalytic activity should be remarkably influenced by the surface properties of the catalysts, so XPS characterization was carried out to determine the surface properties of the supported catalysts, and the Au 4f spectra were shown in Fig. 3. The Au 4f signals of catalysts Au/Al₂O₃ and Au/FeO_x showed at 83.26-83.75 eV and 79.61-80.10 eV, and the binding energy values of Au 4f_{7/2} are fixed 3.1 eV more than those of Au 4f_{5/2}, which is agreed with the binding energy of metallic gold. The aluminium species on the surface of the catalysts were aluminium oxide (Fig. S3D). The Pd 3d peaks were 330.07 eV and 335.60 eV, and it is in line with the binding energy of metallic Pd (Fig. S3A). Meanwhile, the 74.35 eV is the metallic

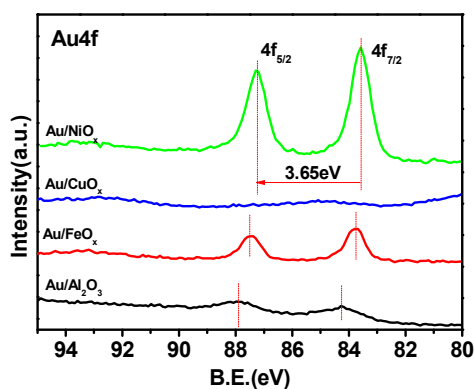


Figure 3. XPS spectra of Au_{4f} of catalysts Au/Al₂O₃, Au/FeO_x, Au/NiO_x and Au/CuO_x.

Pt 4f_{5/2} binding energy, and 284.84 eV is the metallic Ru 3d_{5/2} binding energy (Fig. S3B and C). Nevertheless, weak peaks of gold were found from Au/CuO_x and Au/NiO_x. It suggests that the gold particles might be coated by CuO_x and NiO_x. In addition, the typical binding energy of CuO was found on the surface of Au/CuO_x (Fig. S3G). As metallic copper was observed by XRD characterization, the surface phase composition is

different from the bulk phase. This phenomenon also exists in Au/FeO_x. The surface composition of Au/FeO_x is Au⁰ and Fe₂O₃ (Fig. 3 and Fig. S3E), while it is Fe₃O₄ in the bulk phase, which might be due to the oxidation of catalyst surfaces in the air.

Catalyst screening and reaction conditions optimization

Table 2 shows the results of catalyst screening and reaction conditions optimization with the N-formylation of morpholine as a model reaction at 25 °C in the presence of 1 atm O₂. Clearly, no N-formyl morpholine was formed and the major product was **1c** if Al₂O₃ was used as catalyst directly (Table 2, entry 1). Following, the catalytic performance of catalysts with different noble metals and supports were tested. Clearly, Au/Al₂O₃ exhibits the best catalytic performance, and 96% morpholine conversion with 98% N-formyl morpholine selectivity were obtained. If other catalysts including Pd/Al₂O₃, Ru/Al₂O₃ and Pt/Al₂O₃ were employed, lower conversions or selectivities were obtained (Entries 2-5). Thus supported nano-gold catalyst might be more suitable for the N-formylation of morpholine with paraformaldehyde.

Table 2. Reaction conditions optimization for N-formylation of morpholine^[a]

Entry	Catalyst/mg	Base	Conv. (%) ^[b]	Sel. (%) ^[c]			
				1b	1c	1d	1e
1	Al ₂ O ₃ /25	NaOH	99	3	97	trace	-
2	Pd/Al ₂ O ₃ /20	NaOH	78	93	-	-	7
3	Au/Al ₂ O ₃ /20	NaOH	96	98	2	-	-
4	Ru/Al ₂ O ₃ /20	NaOH	63	26	-	6	68
5	Pt/Al ₂ O ₃ /20	NaOH	68	-	-	34	66
6	Au/FeO _x /20	NaOH	84	31	15	4	50
7	Au/NiO _x /20	NaOH	88	-	11	1	88
8	Au/CuO _x /20	NaOH	64	51	-	20	29
9	Au/Al ₂ O ₃ /5	NaOH	97	25	75	trace	-
10	Au/Al ₂ O ₃ /10	NaOH	95	79	21	trace	-
11	Au/Al ₂ O ₃ /25	NaOH	98	99	-	1	-
12 ^[d]	Au/Al ₂ O ₃ /20	Na ₂ CO ₃	86	79	-	5	16
13 ^[d]	Au/Al ₂ O ₃ /20	K ₂ CO ₃	78	51	-	16	33
14 ^[d]	Au/Al ₂ O ₃ /20	KOH	86	83	-	11	6
15 ^[d]	Au/Al ₂ O ₃ /20	NaOH	74	100	-	-	-
16 ^[d]	Au/Al ₂ O ₃ /20	NaOCH ₃	90	80	-	13	7
17 ^[d]	Au/Al ₂ O ₃ /20	<i>tert</i> -BuOK	98	97	1	1	1
18	Au/Al ₂ O ₃ /25	---	99	9	trace	91	-
19	Au/Al ₂ O ₃ /25	NaOH/2 mg	96	22	trace	78	-
20	Au/Al ₂ O ₃ /25	NaOH/4 mg	96	33	trace	67	-
21	Au/Al ₂ O ₃ /25	NaOH/6 mg	98	96	1	3	-
22	Au/Al ₂ O ₃ /25	NaOH/8 mg	99	99	trace	-	-
23 ^[e]	Au/Al ₂ O ₃ /25	---	79	57	25	-	18

[a] Reaction conditions: **1a** (1.0 mmol), paraformaldehyde (1.2 mmol), catalyst (5-25 mg), NaOH (0.2 mmol), deionized water (2.0 mL), 25 °C, 6 h. [b] Conversion of morpholine was determined by GC-MC. [c] Selectivity by GC-MS analysis based on the morpholine consumed. [d] 25 °C, 4 h. [e] 38% formaldehyde solution (1.2 mmol).



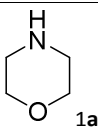
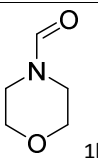
Green Chemistry

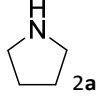
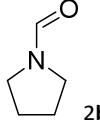
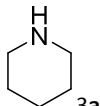
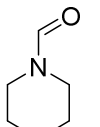
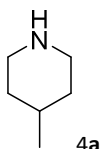
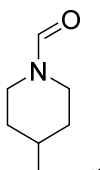
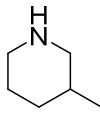
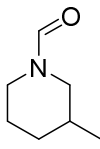
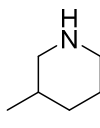
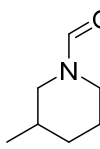
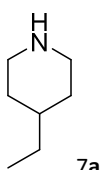
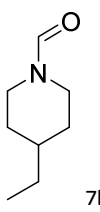
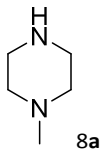
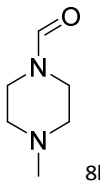
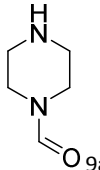
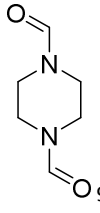
ARTICLE

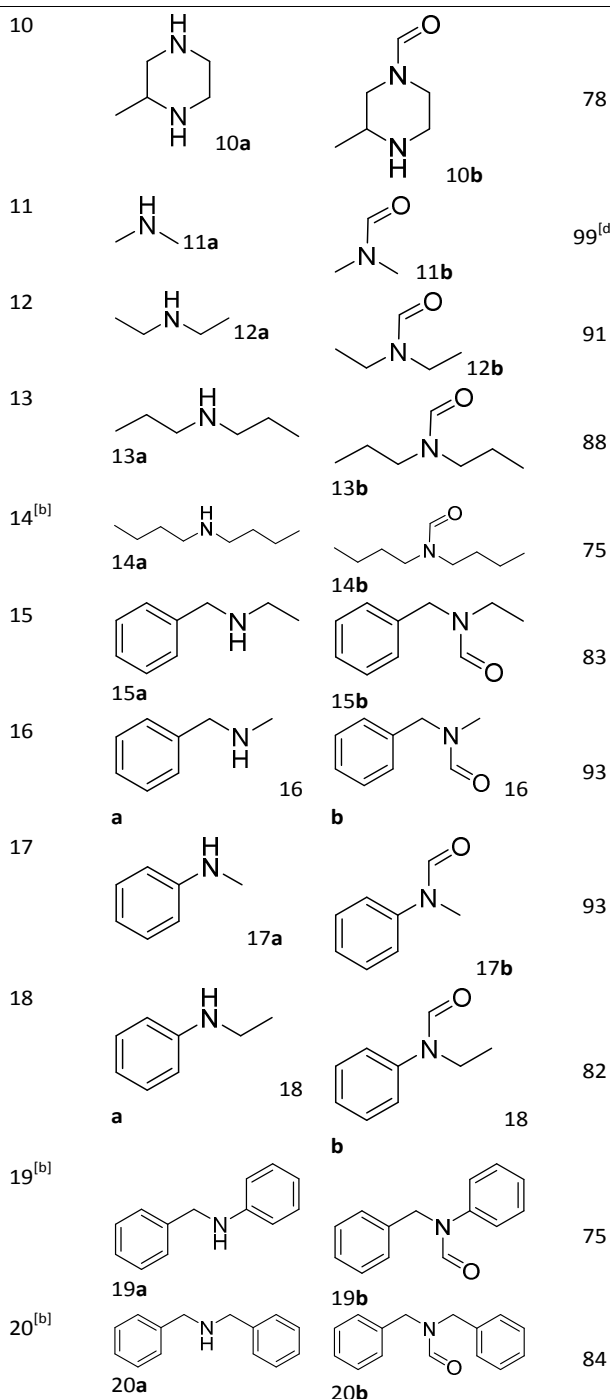
Then, nano-gold catalysts with other supports, i.e., Au/FeO_x, Au/NiO_x and Au/CuO_x were tested. However, the yields to the desired product **1b** were <40% (Entries 6-8). The main reason for their low activity might be attributed to their small surface areas. By applying Au/Al₂O₃ as the model catalyst, the catalyst loadings were varied from 5 mg to 25 mg to check its influence on the catalytic reaction, and finally we found that 97% yield of N-formyl morpholine can be achieved if 25 mg catalyst was added (Entries 3 and 9-11). The influence of base on the catalytic reaction was further tested. Typical bases including Na₂CO₃, K₂CO₃, KOH, NaOH and *tert*-BuOK were tested under the same reaction conditions (Entries 12-17). Although similar conversions of morpholine were observed, it can be seen that 100% selectivity to N-formyl morpholine was obtained if NaOH was used. Thus NaOH is the best cocatalyst for this transformation. Finally the base loadings were tested and the results suggested that 15-20% is the suitable loadings of base (Entries 18-22). The presence of base might promote the depolymerization of paraformaldehyde and nucleophilic addition of amine to formaldehyde (Entries 18, 22 and 23).

Next, the generality of catalyst Au/Al₂O₃ in the N-formylation of different secondary amines with paraformaldehyde were studied (Table 3). For the cyclic secondary amines, including **1a–10a**, the N-formylation products, i.e. **1b–10b**, can be synthesized with 78–97% yields (Entries 1–10 and Scheme 2). The reactions were also successful for the N-formylation of aliphatic secondary amines, and 75%–99% yields of the corresponding products were obtained (Entries 11–16). The applying of secondary amines with aromatic substituents as starting materials should be more challenging due to the weak nucleophilicity of the nitrogen atom. To our delight, excellent results can be achieved with 75-93% isolated yields (Entries 17-18). If secondary amines, i.e., N-benzyl aniline and dibenzyl amine, with melting points above room temperature, the reaction temperature should be increased to 100 °C, and 75-84% isolated yields to the corresponding N-formylation products were obtained, too (Entries 19-20). Therefore, this Au/Al₂O₃ catalyst exhibit nice generality in N-formylation reactions of secondary amines.

Table 3. Results of N-formylation of secondary amines^[a]

Entry	Substrates	Products	Yields ^[c]
1			97

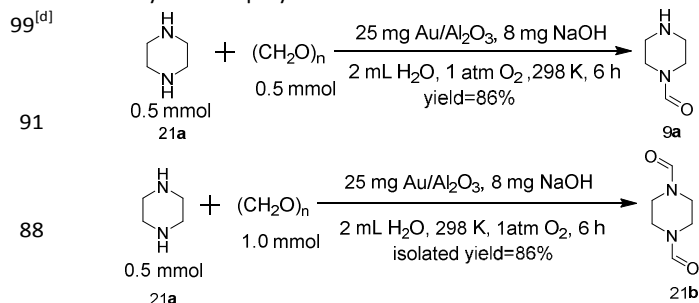
2			88
3			90
4			91
5			78
6			89
7			83
8			92
9			95



[a] Reaction conditions: amine (1.0 mmol), paraformaldehyde (1.2 mmol), catalyst (25 mg), NaOH (0.2 mmol), deionized water (2.0 mL), 25 °C, 6 h. [b] 100 °C, 24 h. [c] Isolated yield. [d] The yields were obtained by GC-FID using biphenyl as the external standard material.

It should be interesting to explore the N-formylation reaction of piperazine because it has two –NH groups so we can check its reactivity for mono- and di-N-formylation reactions (Scheme 2). Clearly, the mono-N-formylation reaction can be realized selectively with 86% yield when 1 equiv., paraformaldehyde was employed, while 1, 4-

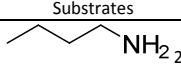
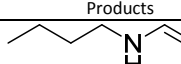
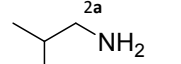
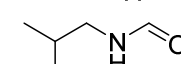
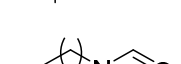
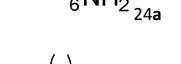
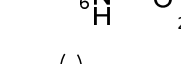
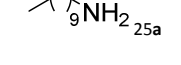
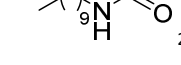
diformylpiperazine can be synthesized with 87% isolated yield when 2 equiv., paraformaldehyde was used. These results indicate that piperazine is more active than the N-formyl piperazine as almost no 1, 4-diformylpiperazine is produced with the addition of 1 equiv., of paraformaldehyde. Therefore, the Au/Al₂O₃ should be a potential catalyst for the selective N-formylation of polyamines.

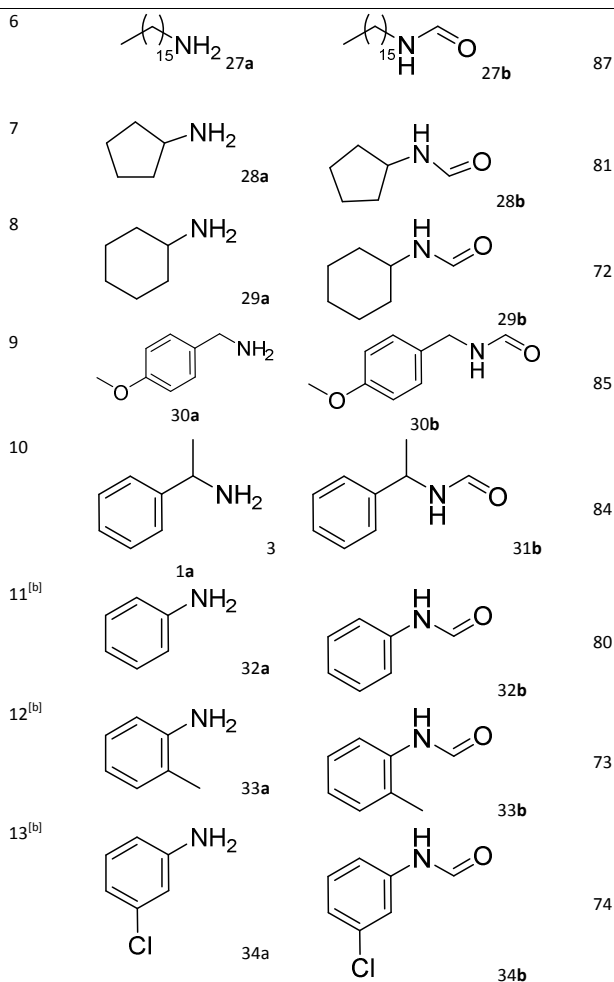


75 Scheme 2. N-formylation of piperazine to synthesis various N-formamine catalyzed by Au/Al₂O₃.

Inspired by the results in Table 3, we further investigated whether N-formamide can be synthesized from primary amines (Table 4). Clearly, butyl amine was converted into N-butylformamide successfully with an isolated yield of 80% (Entry 1). Following, aliphatic primary amines including isobutylamine, 1-heptanamine, 1-decanamine, 1-dodecylamine and 1-cetylamine can be transformed into the corresponding N-formylation products, 23–27b, with yields of 79–87% (Entries 2–6). For cyclic primary amines including cyclopentylamine and cyclohexylamine, the corresponding N-formamides, 28b and 29b, can be synthesized with 81% and 72% isolated yields (Entries 7–8). If benzylamine derivatives with various functional groups, i.e. 30a and 31a, were used as starting materials, the corresponding N-formamides can be obtained selectively with 84% and 85% isolated yields (Entries 9–10). Aniline and aniline derivatives with various functional groups also can be transformed into the corresponding N-formamides with yield of 73%–80% (Entries 11–13). Thus, Au/Al₂O₃ can be used in the N-formylation reactions of primary and secondary amines almost under ambient conditions.

Table 4. Results of N-formylation of primary amines^[a]

Entry	Substrates	Products	Yields ^[c]
1			80
2			82
3			72
4			83
5			79



[a] Reaction conditions: amine (1.0 mmol), paraformaldehyde (1.2 mmol), catalyst (25 mg), NaOH (0.2 mmol), deionized water (2.0 mL), 100 °C, 24 h. [b] 25 °C, 24 h [c] Isolated yield.

Catalyst Reusability

One of the major advantages of heterogeneous catalysts is the facile catalyst separation and recycling. So the reusability of the Au/Al₂O₃ catalyst was tested by the reaction of morpholine with paraformaldehyde (Fig. 4).

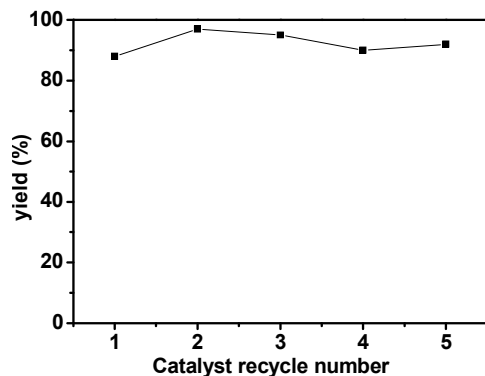


Figure 4. Recyclability test of Au/Al₂O₃ catalyst for the N-formylation of morpholine. Reaction conditions: morpholine (1.0 mmol), paraformaldehyde (1.2 mmol), catalyst (25 mg), NaOH (0.2 mmol), deionized water (2.0 mL), 25 °C, 6 h.

After each reaction, the catalyst was recovered by simple centrifugation and reused without further treatment. As it can be seen from Fig. 4, the catalyst can be recycled for 5 runs without obvious deactivation. As it is well known, supported nano-gold catalysts often face deactivation problem during storage. Thus, it is very interesting to explore the storage stability of the Au/Al₂O₃ catalyst. To our delight, 83% morpholine was converted into N-formyl morpholine with 98% selectivity by applying an Au/Al₂O₃ catalyst being stored in air for 30 days. Thus this catalyst exhibits nice stability during the catalytic reactions, and storage in air.

Catalytic reaction mechanism

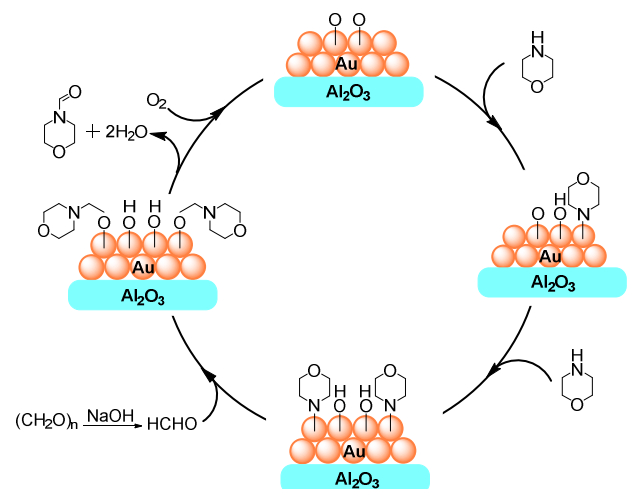
Finally, the reaction mechanism of N-formylation of amine with paraformaldehyde was studied using morpholine as the model substrate. To gain insight into the mechanism, control experiments were conducted under different atmospheres (Table 5). All the reactions were progressed for 6 h and traced by GC-MS. Clearly, morpholine can react with paraformaldehyde to give N-formyl morpholine under 1 atm oxygen in the presence of the Au/Al₂O₃ catalyst. Nevertheless, no N-formyl morpholine was observed under Ar or H₂ atmosphere, and the sole product was aminal 1c. It suggests that the mechanism was oxidative dehydrogenation rather than catalytic dehydrogenation.

Table 5. N-formylation of morpholine under different atmosphere.^[a]

Entry	atmosphere	Conv (%) ^[b]	Sel (%) ^[c]	
			1b	1c
1	O ₂	98	99	-
2	H ₂	65	-	100
3	Ar	78	-	100

[a] Reaction conditions: morpholine (1.0 mmol), paraformaldehyde (1.2 mmol), Au/Al₂O₃ catalyst (25 mg), NaOH (0.2 mmol), deionized water (2.0 mL), 25 °C, 6 h. [b] Conversion of morpholine was determined by GC-MS. [c] Selectivity by GC-MS analysis based on the morpholine consumed.

Based on the former report⁴⁶, a plausible reaction mechanism is given in Scheme 3. First, paraformaldehyde was dissociated in aqueous solution under basic conditions and molecular oxygen was dissociated on the gold-nano particles to form O_{ad}. Then morpholine and dissociated formaldehyde were spread onto the catalyst surface. Morpholine was deprotonated and adsorbed to form adsorbed C₄H₈NO_{ad} and generating water. At the same time formaldehyde was adsorbed to form HCHO_{ad} species. Then, nucleophilic C₄H₈NO_{ad} attacked the aldehydic carbon of formaldehyde, presumably to form the hemiaminal. Subsequently 2-hydride elimination yields N-formyl morpholine. However, the other route cannot be ruled out.



Scheme 3. Plausible reaction pathway for N-formylation of morpholine with paraformaldehyde.

Conclusions

In conclusion, the N-formylation reactions of diffeent amines with paraformaldehyde were achieved successfully catalyzed by a simple Au/Al₂O₃ catalyst. Under the optimized reaction conditions, primary and secondary amines can be efficiently and selectively transformed into the corresponding N-formylation products with excellent yields in water under ambient conditions. It offers a clean and economic method for the synthesis of N-formylation amines.

Acknowledgements

This work was financially supported by the National Natural Science Foundation of China (21203219) and Youth Innovation Promotion Association CAS.

Notes and references

- Y. Zhang, X. Cui, F. Shi and Y. Deng, *Chem. Rev.*, 2011, **112**, 2467-2505.
- A. Corma, A. Leyva-Pérez and M. J. Sabater, *Chem. Rev.*, 2011, **111**, 1657-1712.
- A. Stephen, K. Hashmi and F. D. Toste, *Modern Gold Catalyzed Synthesis*, 2012.
- C. D. Pina, E. Falletta and M. Rossi, *Chem. Soc. Rev.*, 2012, **41**, 350-369.
- J. S. Carey, D. Laffan, C. Thomson and M. T. Williams, *Org. Biomol. Chem.*, 2006, **4**, 2337-2347.
- A. Jackson and O. Meth-Cohn, *J. Chem. Soc., Chem. Commun.*, 1995, 1319-1319.
- V. K. Das, R. R. Devi, P. K. Raul and A. J. Thakur, *Green Chem.*, 2012, **14**, 847-854.
- K. Kobayashi, S. Nagato, M. Kawakita, O. Morikawa and H. Konishi, *Chem. Lett.*, 1995, **24**, 575-576.
- G. Pettit, M. Kalnins, T. Liu, E. Thomas and K. Parent, *J. Org. Chem.*, 1961, **26**, 2563-2566.
- P. C. Wang, X. H. Ran, R. Chen, L. C. Li, S. S. Xiong, Y. Q. Liu, H. R. Luo, J. Zhou and Y. X. Zhao, *Tetrahedron Lett.*, 2010, **51**, 5451-5453.
- C. L. Allen and J. M. J. Williams, *Chem. Soc. Rev.*, 2011, **40**, 3405-3415.
- D. J. C. Constable, P. J. Dunn, J. D. Hayler, G. R. Humphrey, J. J. L. Leazer, R. J. Linderman, K. Lorenz, J. Manley, B. A. Pearlman, A. Wells, A. Zaks and T. Y. Zhang, *Green Chem.*, 2007, **9**, 411-420.
- Gerack and L. McElwee-White, *Molecules*, 2014, **19**, 7689-7713.
- A. Chandra Shekhar, A. Ravi Kumar, G. Sathaiiah, V. Luke Paul, M. Sridhar and P. Shanthan Rao, *Tetrahedron Lett.*, 2009, **50**, 7099-7101.
- M. Hosseini-Sarvari and H. Sharghi, *J. Org. Chem.*, 2006, **71**, 6652-6654.
- J.-G. Kim and D. O. Jang, *Synlett*, 2010, **2010**, 1231-1234.
- H. Lundberg, F. Tinnis, N. Selander and H. Adolfsso, *Chem. Soc. Rev.*, 2014, **43**, 2714-2742.
- I. Sorribes, K. Junge and M. Beller, *Chem. Eur. J.*, 2014, **20**, 7878-7883.
- C. Han, J. P. Lee, E. Lobkovsky and J. A. Porco, *J. Am. Chem. Soc.*, 2005, **127**, 10039-10044.
- B. C. Ranu and P. Dutta, *Synth. Commun.*, 2003, **33**, 297-301.
- C. L. Allen, A. A. Lapkin and J. M. J. Williams, *Tetrahedron Lett.*, 2009, **50**, 4262-4264.
- B. Anxionnat, A. Guérinot, S. Reymond and J. Cossy, *Tetrahedron Lett.*, 2009, **50**, 3470-3473.
- E. Callens, A. J. Burton and A. G. M. Barrett, *Tetrahedron Lett.*, 2006, **47**, 8699-8701.
- A. Goto, K. Endo and S. Saito, *Angew. Chem., Int. Ed.*, 2008, **47**, 3607-3609.
- N. Ibrahim, A. S. K. Hashmi and F. Rominger, *Adv. Synth. Catal.*, 2011, **353**, 461-468.
- S. Ichikawa, S. Miyazoe and O. Matsuoka, *Chem. Lett.*, 2011, **40**, 512-514.
- K. V. Katkar, P. S. Chaudhari and K. G. Akamanchi, *Green Chem.*, 2011, **13**, 835-838.
- S. Murahashi, T. Naota and E. Saito, *J. Am. Chem. Soc.*, 1986, **108**, 7846-7847.
- M. Tamura, H. Wakasugi, K. i. Shimizu and A. Satsuma, *Chem. Eur. J.*, 2011, **17**, 11428-11431.
- M. A. Ali and T. Punniyamurthy, *Adv. Synth. Catal.*, 2010, **352**, 288-292.
- C. L. Allen, C. Burel and J. M. J. Williams, *Tetrahedron Lett.*, 2010, **51**, 2724-2726.
- C. L. Allen, S. Davulcu and J. M. J. Williams, *Org. Lett.*, 2010, **12**, 5096-5099.
- D. Gnanamgari and R. H. Crabtree, *Organometallics*, 2009, **28**, 922-924.
- A. Mishra, A. Ali, S. Upreti and R. Gupta, *Inorg. Chem.*, 2008, **47**, 154-161.
- N. A. Owston, A. J. Parker and J. M. J. Williams, *Org. Lett.*, 2007, **9**, 73-75.
- R. S. Ramón, J. Bosson, S. Díez-González, N. Marion and S. P. Nolan, *J. Org. Chem.*, 2010, **75**, 1197-1202.
- X. Cui, Y. Zhang, Y. Deng and F. Shi, *Chem. Commun.*, 2014, **50**, 189-191.
- L. Zhang, Z. Han, X. Zhao, Z. Wang and K. Ding, *Angew. Chem., Int. Ed.*, 2015, **54**, 6186-6189.
- A. J. A. Watson, A. C. Maxwell and J. M. J. Williams, *Org. Lett.*, 2009, **11**, 2667-2670.
- S. Tanaka, T. Minato, E. Ito, M. Hara, Y. Kim, Y. Yamamoto and N. Asao, *Chem. Eur. J.*, 2013, **19**, 11832-11836.
- K. i. Shimizu, K. Ohshima and A. Satsuma, *Chem. Eur. J.*, 2009, **15**, 9977-9980.
- C. Gunanathan, Y. Ben-David and D. Milstein, *Science*, 2007, **317**, 790-792.
- O. Saidi, M. J. Bamford, A. J. Blacker, J. Lynch, S. P. Marsden, P. Plucinski, R. J. Watson and J. M. J. Williams, *Tetrahedron Lett.*, 2010, **51**, 5804-5806.

Journal Name

ARTICLE

- 44 P. Preedasuriyachai, H. Kitahara, W. Chavasiri and H. Sakurai, *Chem. Lett.*, 2010, **39**, 1174-1176.
- 45 N. Shah, E. Gravel, D. V. Jawale, E. Doris and I. N. N. Namboothiri, *ChemCatChem*, 2014, **6**, 2201-2205.
- 46 B. K. Min and C. M. Friend, *Chem. Rev.*, 2007, **107**, 2709-2724.
- 47 B. Xu, L. Zhou, R. J. Madix and C. M. Friend, *Angew. Chem., Int. Ed.*, 2010, **49**, 394-398.

Supported Nano-Gold-Catalyzed N-Formylation of Amines with Paraformaldehyde in Water under Ambient Conditions

Zhengang Ke, Yan Zhang, Xinjiang Cui, and Feng Shi*

A simple and efficient Au/Al₂O₃ catalyst was prepared for the oxidative N-formylation of amines and paraformaldehyde under ambient conditions with up to 97% yield.

